quence for the cytokine IFN-γ as well. During the course of these studies, Smith *et al.* (*23*) reported that IFN-γ stimulated cytosolic alkalinization in a pre-B lymphocyte cell line, partially as a result of activation of Na^+/H^+ exchange. Because the earliest measured time was 30 min, the rapidity of activated Na^+/H^+ exchange and its importance as a genomic transductional sequence in response to IFN-γ in these cells remain to be established. In view of the pleotropic actions of IFN-γ (*5, 6*), it is likely that additional transductional sequences may mediate other actions of IFN-γ. For instance, addition of amiloride did not inhibit priming by IFN-γ for tumor cell cytolysis (*9*). Relatively high concentrations of IFN-γ can cause accumulation of labeled diacylglycerol or similar compounds in fibroblasts (*24*). In macrophages, physiologic concentrations of IFN-γ, however, induce increases in the mass of diacylglycerol only after ~4 hours, suggesting that these increases are unlikely to represent a primary transductional event (*25*). Our studies demonstrate that physiologic doses of IFN-γ induce rapid Na^+/H^+ exchange in murine macrophages and that these amiloride-sensitive fluxes are important for mediating some of the subsequent genomic responses to IFN-γ.

REFERENCES AND NOTES

1. S. Pestka, J. A. Langer, K. C. Zoon, C. E. Samuel, *Annu. Rev. Biochem.* **56**, 727 (1987).
2. D. O. Adams and T. A. Hamilton, in *Inflammation: Basic Principles and Clinical Correlates*, J. I. Gallin, I. M. Goldstein, R. Snyderman, Eds. (Raven, New York, 1988), pp. 471–492.
3. E. R. Unanue, *Annu. Rev. Immunol.* **2**, 395 (1984).
4. D. O. Adams and T. A. Hamilton, *ibid.*, p. 283.
5. ———, *Immunol. Rev.* **97**, 5 (1987).
6. T. A. Hamilton and D. O. Adams, *Immunol. Today* **8**, 151 (1987).
7. S. D. Somers, J. E. Weiel, T. A. Hamilton, D. O. Adams, *J. Immunol.* **136**, 4199 (1986).
8. C. Frelin, P. Vigne, P. Barbry, M. Lazdunski, *Kidney Int.* **32**, 785 (1987); T. R. Kleyman and E. J. Cragoe, Jr., *J. Membr. Biol.* **105**, 1 (1988).
9. V. Prpic *et al.*, unpublished observations.
10. T. J. Koerner and D. O. Adams, *Year Imunol.* **4**, 1 (1988); F. Figueiredo-Neto, T. J. Koerner, D. O. Adams, in preparation; D. Fertsch-Ruggio, D. Schoenberg, S. N. Vogel, *J. Immunol.* **141**, 1582 (1988); F. M. Rosa and N. Fellous, *ibid.* **140**, 1660 (1988).
11. T. J. Koerner *et al.*, *Biochem. Biophys. Res. Commun.* **149**, 969 (1987).
12. M. Introna *et al.*, *J. Immunol.* **138**, 3891 (1987).
13. T. J. Koerner *et al.*, *ibid.* **139**, 239 (1987).
14. B. H. Cochran, *et al.*, *Cell* **33**, 939 (1983).
15. B. J. Rollins, E. D. Morrison, C. D. Stiles, *Proc. Natl. Acad. Sci. U.S.A.* **85**, 3738 (1988).
16. D. J. Hall and C. D. Stiles, *J. Biol. Chem.* **262**, 15302 (1987).
17. R. A. Flavell *et al.*, *Science* **233**, 437 (1986).
18. M. Revel and J. Chebeth, *Trends Biochem. Sci.* **11**, 166 (1986).
19. T. A. Hamilton, P. V. Gainey, D. O. Adams, *J. Immunol.* **138**, 4063 (1987).
20. V. Prpic *et al.*, in preparation.
21. E. Rozengurt, *Science* **234**, 161 (1986).
22. W. H. Moolenaar, *Annu. Rev. Physiol.* **48**, 363 (1986).
23. L. L. Smith, T. H. Stanton, M. B. Calalb, K. Bomsztyk, *J. Biol. Chem.* **263**, 7359 (1988).
24. W. H. Yap *et al.*, *Science* **234**, 355 (1986).
25. R. J. Sebaldt *et al.*, in preparation.
26. T. J. Rink *et al.*, *J. Cell Biol.* **95**, 189 (1982).
27. B. Herman *et al.*, *Cell Motil. Cytoskeleton* **8**, 91 (1987).
28. Proteose-peptone–elicited macrophages were obtained by peritoneal lavage of pathogen-free 6-week-old inbred C57BL/6 mice (Charles River). Macrophages (1 ml containing 1×10^6 cells) were cultured for 5 hours at 37°C with 5% CO_2 on glass cover slips (22 mm by 22 mm) in RPMI 1640 containing 5% fetal calf serum, 2 m*M* glutamine, penicillin (125 U/ml), and streptomycin (6.25 μg/ml). Cultures were incubated for 30 min with BCECF-acetoxymethyl ester (2 μ*M*), and then washed three times in HHBSS. The cover slips with macrophage monolayers were then placed in a similar medium on the stage of an inverted-phase fluorescent microscope. Fluorescence of the individual cells was then measured with the use of a digitized video microscopy system described elsewhere (*26, 27*), with the following filter combination: excitation 440 or 490 nm, emission >525 nm. Values of pH_i were obtained by comparing 440/490 ratios with those obtained with BCECF-containing solutions of known *p*H. Similar pH_i values were obtained for nigericin-permeabilized (*26*) BCECF-containing cells. For $^{22}Na^+$ influx measurements, 6×10^6 peptone-elicited adherent macrophages were in modified Hanks balanced salt solution with 14 m*M* NaCl, 123 m*M* choline chloride, and 5 m*M* Na/Hepes, *p*H 7.4. Cells were warmed at 37°C for 10 min before the addition of 0.5 m*M* ouabain or ouabain plus the indicated concentrations of amiloride and then kept at 37°C for an additional 5 min. At the end of the preincubation, either buffer or IFN-γ plus 2 μCi of $^{22}Na^+$ per well was added for the indicated times after which the wells were washed five times with 0.1*M* $MgCl_2$ at 4°C during a 1-min period. Monolayers were solubilized with 1*N* NaOH and counted in a gamma counter. Efficiency of counting was ~50%.
29. J. M. Chirgwin, A. E. Przybyla, R. J. MacDonald, W. I. Rutter, *Biochemistry* **18**, 5294 (1979).
30. P. S. Thomas, *Methods Enzymol.* **100**, 255 (1983).
31. G. M. Church and W. Gilbert, *Proc. Natl. Acad. Sci. U.S.A.* **81**, 1991 (1984).

32. We thank E. J. Cragoe, Jr., for providing the amiloride analogs 5-(*N*-methyl-*N*-isobutyl)amiloride and 5-[*N*-methyl-*N*-(amidinocarbonylmethyl)] amiloride. Supported by USPHS (D.O.A., B.H., and R.J.U.), RJR/Nabisco (D.O.A.), the American Heart Association (B.H.), the Pfeiffer Foundation (B.H.), and the National Council of Scientific and Technological Development, Brazil (F.F.).

31 October 1988; accepted 14 February 1989

High Rate of HTLV-II Infection in Seropositive IV Drug Abusers in New Orleans

HELEN LEE, PRISCILLA SWANSON, VERNON S. SHORTY, JEROME A. ZACK, JOSEPH D. ROSENBLATT, IRVIN S. Y. CHEN

Confirmed infection with HTLV-II (human T cell leukemia virus type II) has been described only in rare cases. The major limitation to serological diagnosis of HTLV-II has been the difficulty of distinguishing HTLV-II from HTLV-I (human T cell leukemia virus type I) infection, because of substantial cross-reactivity between the viruses. A sensitive modification of the polymerase chain reaction method was used to provide unambiguous molecular evidence that a significant proportion of intravenous drug abusers are infected with HTLV, and the majority of these individuals are infected with HTLV-II rather than HTLV-I. Of 23 individuals confirmed by polymerase chain reaction analysis to be infected with HTLV, 21 were identified to be infected with HTLV-II, and 2 were infected with HTLV-I. Molecular identification of an HTLV-II–infected population provides an opportunity to investigate the pathogenicity of HTLV-II in humans.

HUMAN T CELL LEUKEMIA VIRUSES type I (HTLV-I) and type II (HTLV-II) have been associated with specific forms of malignancy in humans. HTLV-I is the etiologic agent for a malignancy known as adult T cell leukemia (*1*) and has been linked to a chronic myelopathy known as HTLV-I–associated myelopathy (*2*) or tropical spastic paraparesis, which is endemic to regions of Japan, the Caribbean, and Africa (*3*). Sporadic cases of HTLV-I infection have also been reported in other areas in the world; in the United States, it has been particularly observed in the southeastern region (*4*). Recently, HTLV-seropositive individuals were identified among an intravenous (IV) drug abuser population (*5*), but infection has not been confirmed by more stringent criteria.

In contrast to HTLV-I, HTLV-II has only rarely been isolated. HTLV-II has been associated with two cases of malignancy in humans (*6*). Both patients had unusual T cell malignancies resembling hairy-cell leukemia. In one case, we showed definitively that HTLV-II was molecularly associated with a lymphoproliferative disorder involv-

H. Lee and P. Swanson, Diagnostics Division, Abbott Laboratories, North Chicago, IL 60064.
V. S. Shorty, Desire Narcotics Rehabilitation Center, New Orleans, LA 70126.
J. A. Zack and I. S. Y. Chen, Department of Microbiology and Immunology, and Division of Hematology-Oncology, Department of Medicine, Jonsson Comprehensive Cancer Center and UCLA School of Medicine, Los Angeles, CA 90024.
J. D. Rosenblatt, Division of Hematology-Oncology, Department of Medicine, Jonsson Comprehensive Cancer Center, and UCLA School of Medicine, Los Angeles, CA 90024.

ing a clonal $CD8^+$ population of cells. HTLV-II has also been isolated in rare cases from individuals without evidence of malignancy, including a hemophiliac with unexplained pancytopenia and a patient with acquired immunodeficiency syndrome (AIDS) (7). The low number of cases of HTLV-II infection has made it difficult to establish conclusively an association with or a causative role for HTLV-II in a specific disease. In one serological study in New York, a significant proportion of those cases with HTLV-reactive antibodies were thought to be due to HTLV-II infection (*5*). In another study of IV drug abusers in Great Britain (*8*), infection of a proportion of these individuals was also attributed to HTLV-II. In each of these studies, the differentiation between HTLV-I and HTLV-II was based on competition enzyme-linked immunosorbent assays. Because of the relatively high amino acid sequence homology (*9, 9a*), resulting in substantial cross-reactivity between HTLV-I and HTLV-II, and the relatively few cases of HTLV-II infection with which to establish specificity, it was not conclusively established that HTLV-II infection was present among these populations. Molecular methods for HTLV detection would be the most rigorous; however, this means of detection has not been possible in asymptomatic individuals because of the low proportion of infected cells. Thus, previous methods for molecular discrimination by DNA blotting have required lengthy culture of patient lymphocytes and have not allowed detection of HTLV-I or HTLV-II in fresh samples. In this study, we have used a modification of the polymerase chain reaction (PCR) (*10*) method to detect HTLV-I and HTLV-II infection directly in DNA obtained from fresh blood samples. This modified method is sensitive and rapid, and it can be used to easily discriminate between HTLV-I and HTLV-II infection. We determined that the majority of HTLV-seropositive individuals in an IV drug abuser population in New Orleans are infected with HTLV-II rather than HTLV-I.

```
                7248
HTLV-II:  TGGATACCCCGTCTACGTGTTTGGCGATTGTGTACAGGCCGATTGGTGTCCCGTCTCAGGTGGTCTATGTTCCACCCGC

                7336
HTLV-I:   CGGATACCCAGTCTACGTGTTTGGAGACTGTGTACAAGGCGACTGGTGCCCCATCTCTGGGGGACTATGTTCGGCCCGC


                7327  ↓Taq I                                          ↓Taq I
HTLV-II:  CTACATCGACATGCCCTCCTGGCCACCTGTCCAGAGCACCAACTCACCTGGGACCCCATCGATGGACGCGTTGTCAGCTC

                7415                                    ↓Sau 3A         ↓Taq I
HTLV-I:   CTACATCGTCACGCCCTACTGGCCACCTGTCCAGAGCATCAGATCACCTGGGACCCCATCGATGGACGCGTTATCGGCTC
```

Fig. 1. Nucleotide sequence of the HTLV-I and HTLV-II *tax/rex* gene region. The published nucleotide sequence of HTLV-I (*9a*) and HTLV-II (*9*) proviral clones is shown for the region of *tax/rex* genes chosen for PCR amplification. The HTLV-I and HTLV-II sequences are aligned. Nucleotide numbers are those indicating the position in an entire proviral clone. The position of relevant restriction enzyme sites Taq I and Sau 3A are indicated by arrows, and the position of the primers (*15*) used for PCR amplification are underlined. The upstream oligonucleotide primer was labeled at the 5′ end with [γ-^{32}P]ATP in all experiments.

Table 1. HTLV-I and HTLV-II infection among IV drug abusers in New Orleans. The HTLV-I EIA is manufactured by Abbott Laboratories. A negative result means less than 4.5 times the optical density reading of the negative control, which consists of pooled normal human sera supplied with the EIA. Protein immunoblotting against HTLV-I virion antigens and RIPA with [^{35}S]methionine and cysteine-labeled infected cell lysates were used for confirmation of reactivity. A seropositive result by protein immunoblotting and RIPA was determined only when both gp46/gp61 (*env*) and p24 (*gag*) were reactive. Those samples confirmed by protein immunoblotting or RIPA are indicated as positive by serology. PCR analysis was performed as indicated (*13*). All samples were screened with *tax/rex*–specific primers, and discrimination of HTLV-I and HTLV-II was performed by restriction enzyme digestion with Sau 3A or Taq I, as indicated (*13*) (Fig. 3). Samples 338, 782, 28, 221, 1160, 48, 1079, 983, 151, 334, 1419, 1287, and 1259 were reanalyzed on a separate occasion with fresh blood samples. Samples 975, 338, 782, 221, 28, 1160, 48, 1079, 983, 151, 334, 1419, 1259, 36, 18, 1287, 1038, 315, 1296, and 611 were tested for HTLV-I or HTLV-II with the use of primer pairs from *pol* that hybridize only with HTLV-I; as expected, of these, only sample 975 tested positively for HTLV-I. Similarly, samples 782, 1160, 1079, 151, 1419, 1259, 36, and 18 were confirmed positive for HTLV-II with the use of HTLV-II–specific primers from *pol*. Samples 782, 1160, 1419, and 975 were further confirmed by nucleotide sequence analysis (Fig. 4). IND, indeterminate.

Sample code	HTLV-I EIA	Protein immuno-blot	RIPA	Serol-ogy result	PCR result	
					HTLV-I	HTLV-II
338	+	+	+	+	−	+
782	+	IND	+	+	−	+
28	+	+	+	+	−	+
1160	+	IND	+	+	−	+
48	+	IND	+	+	−	+
1079	+	IND	+	+	−	+
86	+	+	+	+	−	+
151	+	IND	+	+	−	+
1419	+	+	+	+	−	+
1259	+	IND	+	+	−	+
308	+	IND	+	+	−	+
41	+	IND	+	+	−	+
1038	+	IND	+	+	−	+
36	+	IND	+	+	−	+
611	+	IND	+	+	−	+
64	+	IND	+	+	−	+
983	+	IND	IND	IND	−	+
27	+	IND	−	IND	−	+
18	+	IND	−	IND	−	+
334	+	−	−	−	−	+
13	−	−	−	−	−	+
310	+	IND	+	+	+	−
975	+	+	+	+	+	−
1296	+	IND	−	IND	−	−
221	−	−	−	−	−	−
1287	−	−	−	−	−	−
315	−	−	−	−	−	−

Blood samples were obtained from IV drug abusers in New Orleans. Initially, serum was screened for antibodies to HTLV-I by enzyme immunoassay (EIA) (Abbott Laboratories). Although purified disrupted HTLV-I virions were used in the EIA, sera from two previously identified individuals infected with HTLV-II isolates [HTLV-II_{Mo} and HTLV-II_{NRA} (*6*)] were strongly cross-reactive in the HTLV-I EIA assay. Therefore, this assay would be expected to react with other HTLV-II antibody–positive sera. Of 121 samples screened, 54 were positive by EIA. These samples were further tested for reactivity against HTLV-I or HTLV-II antigens by protein immunoblotting (*11*) and by radioimmunoprecipitation assay (RIPA) (*12*) analysis, with the use of the HTLV-I–infected cell line HUT 102-B2 and the HTLV-II–infected cell line 729pH6neo. Thirty-three of the 54 samples were confirmed to be seropositive by pro-

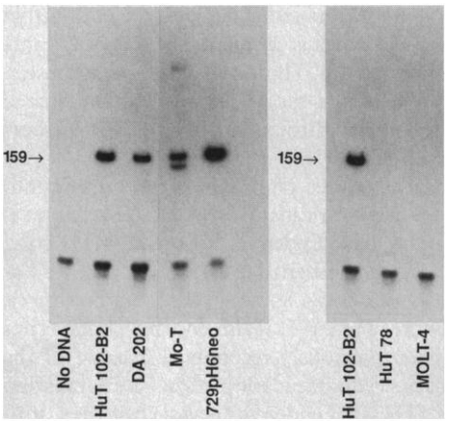

Fig. 2. Specificity of PCR assay for HTLV sequences. Analysis of samples for HTLV sequences after 30 cycles of PCR amplification was as described (*13*). The labeled PCR products were analyzed by electrophoresis on 8% polyacrylamide gels (1.5 mm, 100 volts, 4 hours) and then autoradiography was performed. HUT 102-B2 and DA 202 are HTLV-I–infected cell lines; Mo-T and 729pH6neo are HTLV-II–infected cell lines; and HUT 78 and MOLT-4 are uninfected cell lines. Ten nanograms of DNA of each HTLV-infected cell, and 2 μg of other DNAs were analyzed. The position of the 159-nt HTLV-specific amplified DNA product is indicated. Mo-T consistently shows an additional band slightly smaller than the 159-nt product. This product is due to defective HTLV-II proviruses in the Mo-T cells. The lower band in all lanes represents the position of labeled oligonucleotide, which was not incorporated into amplified products.

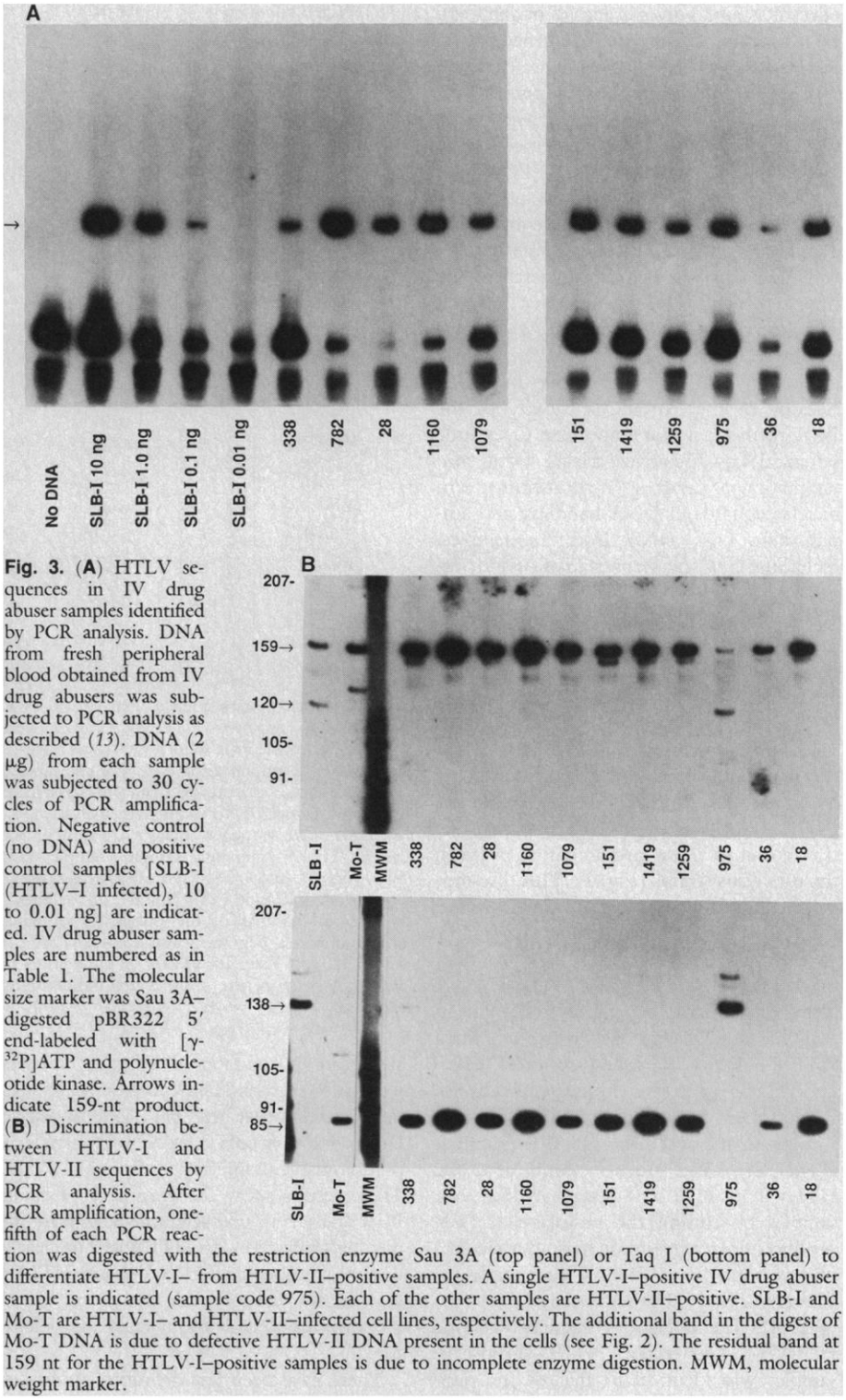

Fig. 3. (**A**) HTLV sequences in IV drug abuser samples identified by PCR analysis. DNA from fresh peripheral blood obtained from IV drug abusers was subjected to PCR analysis as described (*13*). DNA (2 μg) from each sample was subjected to 30 cycles of PCR amplification. Negative control (no DNA) and positive control samples [SLB-I (HTLV–I infected), 10 to 0.01 ng] are indicated. IV drug abuser samples are numbered as in Table 1. The molecular size marker was Sau 3A–digested pBR322 5′ end-labeled with [γ-^{32}P]ATP and polynucleotide kinase. Arrows indicate 159-nt product. (**B**) Discrimination between HTLV-I and HTLV-II sequences by PCR analysis. After PCR amplification, one-fifth of each PCR reaction was digested with the restriction enzyme Sau 3A (top panel) or Taq I (bottom panel) to differentiate HTLV-I– from HTLV-II–positive samples. A single HTLV-I–positive IV drug abuser sample is indicated (sample code 975). Each of the other samples are HTLV-II–positive. SLB-I and Mo-T are HTLV-I– and HTLV-II–infected cell lines, respectively. The additional band in the digest of Mo-T DNA is due to defective HTLV-II DNA present in the cells (see Fig. 2). The residual band at 159 nt for the HTLV-I–positive samples is due to incomplete enzyme digestion. MWM, molecular weight marker.

tein immunoblotting or RIPA. A subset of these individuals was further analyzed (Table 1).

To distinguish between HTLV-I and HTLV-II infection in these individuals, we used a simplified adaptation of the PCR method for detection of viral nucleic acids (*13*). This modification involved the radioactive labeling of the 5′ end of one oligonucleotide of the primer pair with [γ-^{32}P]adenosine triphosphate (ATP). Conditions for PCR were optimized to minimize background and maximize sensitivity. The method is rapid because PCR amplification products can be directly visualized after acrylamide gel electrophoresis and autoradiography. Therefore, subsequent hybridization steps, which may lead to further variability, are eliminated. Confirmation of the specificity of the PCR products can be performed by digestion with specific restriction enzymes that will differentiate between the PCR products of HTLV-I and HTLV-II or by direct sequence analysis of the radiolabeled products (*14*).

For initial screening, sequences were chosen from HTLV-I and HTLV-II *tax/rex* regions that had sufficient similarity to allow detection of either viral DNA (*15*); use of these primers resulted in a PCR product of 159 nucleotides (nt) (Fig. 1). The specificity of the PCR primers was demonstrated by the presence of 159-nt products in nine HTLV-I– and HTLV-II–infected cell lines tested (Fig. 2, four cell lines shown), whereas four uninfected cell lines (Fig. 2, two cell lines shown) and two HIV-infected cell lines were negative. Serial dilutions of DNA from HTLV-I– or HTLV-II–infected cells followed by PCR amplification resulted in a dose-dependent detection of HTLV DNA. In experiments (Fig. 3A) in which the HTLV-I–infected cell line SLB-I was used, the equivalent of about ten infected cells (0.1 ng) was easily detected.

PCR analysis was performed in a blind study on 27 samples from IV drug abusers tested for seropositivity for HTLV-I or HTLV-II by EIA, protein immunoblot, and RIPA (Table 1 shows complete compilation

of results; Fig. 3 gives examples of analysis). Of this group, 18 were confirmed to be seropositive, 4 were indeterminate (positive by EIA, but not confirmed by protein immunoblot or RIPA), and 5 were seronegative. All of the samples confirmed to be seropositive were also positive by PCR analysis. Of the nine seronegative or indeterminate samples, five were positive by PCR, and four were negative. One sample (sample code 13) that was negative by each of the three serologic criteria was positive by PCR, and another sample (sample code 334) positive by EIA but negative by protein immunoblot and RIPA was positive by PCR. Because of the extreme sensitivity of the PCR method, it was important to exclude potential false positives arising from contamination of samples. In addition to technical safeguards in DNA handling and amplification (*13*), DNA from 13 samples, including 4 of the seronegative or indeterminate samples, was retested on a separate occasion after a repeat blood draw several months after the initial analysis. As an added precaution, the lymphocytes were isolated at a separate location from the initial samples. The results of these samples were identical.

Different isolates of HTLV-I or HTLV-II show little nucleotide sequence heterogeneity within the *tax/rex* region (*16*). However, HTLV-I and HTLV-II differ sufficiently in this region to allow discrimination between the two virus strains (Fig. 1). This discrimination could be achieved by digesting the PCR products with the appropriate restriction enzyme after the PCR amplification. Sau 3A cleaves the amplified HTLV-I DNA to generate a labeled fragment of 120 nt in size, but it does not cleave the amplified HTLV-II DNA. Taq I digests both HTLV-I and HTLV-II in the region spanned by the PCR primers but results in a 138-nt HTLV-I fragment and an 85-nt HTLV-II fragment (Fig. 3B). We further confirmed the HTLV-I or HTLV-II specificity for four samples by eluting the radiolabeled PCR products from acrylamide gels after electrophoresis and by subjecting the samples to Maxam-Gilbert DNA sequence analysis (*14*) (Fig. 4). The nucleotide sequence of one HTLV-I– and three HTLV-II–positive samples was identical to that of the published sequence of HTLV-I and HTLV-II, respectively. In addition, 20 samples (Table 1) were further confirmed by use of PCR primers from the *pol* gene region, which specifically detect either HTLV-I or HTLV-II DNA. Of the 23 samples determined to be positive for either HTLV-I or HTLV-II by PCR, only two were positive for HTLV-I. No samples were identified that harbored sequences of both HTLV-I and HTLV-II. Thus, the PCR analysis confirms that a

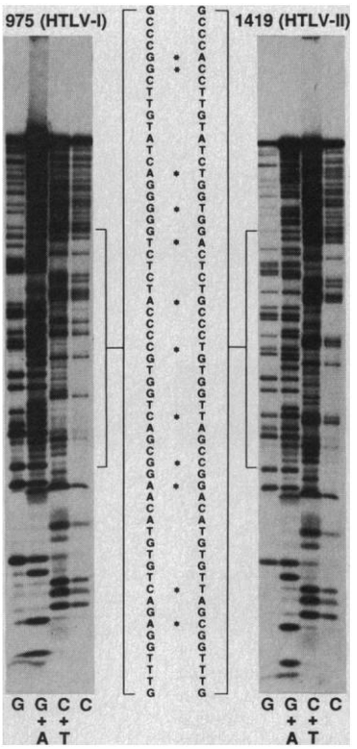

Fig. 4. Nucleotide sequence analysis of PCR amplification products. Selected samples were subjected to nucleotide sequence analysis after 40 cycles of PCR amplification (*13*). The end-labeled PCR products were excised from polyacrylamide gels and subjected to sequence analysis (*14*). Representative sequence analyses are shown, one for an HTLV-I–positive sample (sample code 975, Fig. 3), and one for an HTLV-II–positive sample (sample code 1419, Fig. 3). The sequence is identical to that of the published sequence shown in Fig. 1, beginning at nucleotide 7267 for HTLV-II and 7355 for HTLV-I. Differences in sequence between the samples are indicated by asterisks.

significant proportion of IV drug abusers were infected with HTLV and demonstrates unexpectedly that the HTLV-seropositive IV drug abuser cohort in New Orleans was predominantly infected with HTLV-II. These results show the feasibility of using PCR analysis to unambiguously identify individuals infected with HTLV and to clearly discriminate between HTLV-I and HTLV-II with the use of fresh peripheral blood mononuclear cells without resorting to culture.

There have been few definitive reports of HTLV-II infection, and no endemic region for this virus has been identified. It is, therefore, of interest that the majority of the cases in our study are HTLV-II. Clearly, HTLV-II has the same capacity as HTLV-I to spread, once it is introduced into the appropriate population—in this case, an IV drug abuser population. HTLV-II is readily transmitted (in the laboratory) to uninfected cells by cocultivation with infected cells, as has been seen with HTLV-I (*17*). Epidemiologic studies indicate that transfer of viable infected cells is required for HTLV-I transmission (*18*). Thus, among IV drug abusers, HTLV-II is most likely spread by shared needle use through transfer of cells harboring HTLV-II.

The source of HTLV-II introduced into the New Orleans drug abuser population is unknown. Endemic regions for HTLV-I include southern Japan, Africa, and the Caribbean (*1–3*). Some of these may be regions where HTLV-II is also endemic, but has not been previously recognized because of the lack of discriminating tests. Reexamination of HTLV-I endemic areas such as the Caribbean basin will be important. Furthermore, the unusually high rate of HTLV-II infection and the detection of one individual seronegative by three serologic criteria but determined as infected by PCR analysis (Table 1, sample code 13) underscore the importance of further comparisons among molecular and serological screening methods.

Although the individuals studied here are apparently asymptomatic, the long latency period associated with diseases of HTLV-I infection would suggest that hematologic, immunologic, or neurologic complications of HTLV-II infection may develop with time. Thus, it is critical that prospective epidemiological and clinical analyses of this HTLV-II–infected population be performed to understand the natural history and pathogenesis of HTLV-II.

REFERENCES AND NOTES

1. T. Uchiyama *et al.*, *Blood* **50**, 481 (1977); B. J. Poiesz *et al.*, *Proc. Natl. Acad. Sci. U.S.A.* **77**, 7415 (1980); Y. Hinuma *et al.*, *ibid.* **78**, 6476 (1981); M. Yoshida *et al.*, *ibid.* **79**, 2031 (1982).
2. A. Gessain *et al.*, *Lancet* **ii**, 407 (1985); M. Osame *et al.*, *ibid.* **i**, 1031 (1986).
3. R. J. Biggar *et al.*, *Int. J. Cancer* **35**, 763 (1985); W. A. Blattner *et al.*, *ibid.* **30**, 257 (1982); D. Catovsky *et al.*, *Lancet* **i**, 639 (1982); S. Merl *et al.*, *Blood* **64**, 967 (1984); W. Saxinger *et al.*, in *Human T-Cell Leukemia/Lymphoma Virus*, R. C. Gallo, Ed. (Cold Spring Harbor Laboratory, Cold Spring Harbor, NY, 1984), pp. 323–330; I.-J. Su *et al.*, *Cancer* **56**, 2217 (1985).
4. D. W. Blayney *et al.*, *Blood* **62**, 401 (1983); P. A. Bunn, Jr., *et al.*, *N. Engl. J. Med.* **309**, 257 (1983).
5. M. Robert-Guroff *et al.*, *J. Am. Med. Assoc.* **255**, 3133 (1986).
6. V. S. Kalyanaraman *et al.*, *Science* **218**, 571 (1982); A. Saxon *et al.*, *Ann. Intern. Med.* **88**, 323 (1978); J. D. Rosenblatt *et al.*, *Blood* **71**, 363 (1988); J. D. Rosenblatt *et al.*, *N. Engl. J. Med.* **315**, 372 (1986).
7. B. H. Hahn *et al.*, in *Acquired Immune Deficiency Syndrome*, M. S. Gottlieb and J. E. Groopman, Eds. (Liss, New York, 1984), pp. 73–81; V. S. Kalyanaraman *et al.*, *EMBO J.* **4**, 1455 (1985).
8. R. S. Tedder *et al.*, *Lancet* **ii**, 125 (1984).
9. K. Shimotohno *et al.*, *Proc. Natl. Acad. Sci. U.S.A.* **82**, 3101 (1985).

9a. M. Seiki, S. Hattori, Y. Hirayama, M. Yoshida, *ibid.* **80**, 3618 (1983).

10. R. K. Saiki *et al.*, *Science* **230**, 1350 (1985).
11. H. Towbin, T. Stachelin, J. Gordon, *Proc. Natl. Acad. Sci. U.S.A.* **76**, 4350 (1979).
12. D. D. Ho *et al.*, *Science* **239**, 1021 (1988).
13. Heparinized blood samples were obtained (after

informed consent from IV drug abusers in New Orleans who were attending the Desire Narcotics Rehabilitation Center), and peripheral blood mononuclear cells were isolated by Ficoll-Hypaque density gradient centrifugation (at UCLA and Abbott Laboratories). The peripheral blood mononuclear cells were cryopreserved until further analysis. Preparation of all blood samples and storage were performed with the use of facilities and reagents specifically designated for PCR analysis. DNA was prepared from approximately 10^7 cryopreserved cells by SDS–proteinase K treatment, followed by phenol and chloroform extraction. DNA was analyzed by PCR (*10*) with the following modification. Samples were subjected to PCR analysis for 30 cycles (40 cycles for DNA sequence analysis) with 100 ng of each primer, including 5×10^6 cpm of one primer labeled at the 5′ end with [γ-^{32}P]ATP. Reactions were performed in 25 m*M* tris-HCl, *p*H 8.0, 5 m*M* $MgCl_2$, 50 m*M* NaCl, and 0.25 m*M* each of deoxyadenosine triphosphate, deoxycytidine triphosphate, deoxythymidine triphosphate, and deoxyguanosine triphosphate in a total volume of 25 μl, cycling at 65°C for 2 min and at 91°C for 1 min. After amplification, 5 μl of the reaction were used for further analysis by 8% polyacrylamide gel electrophoresis. With these modifications, the PCR products could be visualized directly after gel electrophoresis and autoradiography, without a need for additional hybridization steps. Exposure times varied from 2 to 12 hours, depending on the intensity of the signal. Oligonucleotide primers corresponding to the *tax/rex* region of HTLV-I were used to detect both HTLV-I and HTLV-II sequences. Oligonucleotides from the *pol* gene region that specifically detect either HTLV-I or HTLV-II were also tested in some cases. The possibility of false positives because of the extreme sensitivity of the PCR method was excluded for the following reasons: (i) DNA preparation and PCR reactions were performed in a separate facility from the location where the PCR products were analyzed. (ii) All reagents were specifically designated for PCR analysis and used exclusively for that purpose. (iii) Negative control samples were included in parallel at each step, from purification of blood mononuclear cells through PCR analysis. (iv) Results from some samples were confirmed with a second lymphocyte isolation and prepared in geographically distinct laboratories.

14. A. M. Maxam and W. Gilbert, *Proc. Natl. Acad. Sci. U.S.A.* **74**, 560 (1977).
15. D. B. Duggan *et al.*, *Blood* **71**, 1022 (1988); S. Bhagavati *et al.*, *N. Engl. J. Med.* **318**, 1141 (1988).
16. K. T. A. Malik, J. Eveir, A. Karpas, *J. Gen. Virol.* **69**, 1695 (1988); L. Ratner, *J. Virol.* **54**, 781 (1985); H. Tsujimoto, *Mol. Biol. Med.* **5**, 29 (1988); HTLV-II_{Mo} and HTLV-II_{NRA} show 99% homology in the long terminal repeat (I. S. Y. Chen and J. D. Rosenblatt, unpublished data).
17. I. S. Y. Chen *et al.*, *Proc. Natl. Acad. Sci. U.S.A.* **80**, 7006 (1983); T. N. Chosa *et al.*, *Gann* **73**, 844 (1982); I. Miyoshi *et al.*, *ibid.* **72**, 997 (1981); M. Popovic *et al.*, *Proc. Natl. Acad. Sci. U.S.A.* **80**, 5402 (1983); N. Yamamoto *et al.*, *Science* **217**, 737 (1982).
18. J. M. Jason, J. S. McDougal, C. Cabradilla, V. S. Kalyanaraman, B. L. Evatt, *Am. J. Hematol.* **20**, 129 (1985); G. Y. Minamoto *et al.*, *N. Engl. J. Med.* **318**, 219 (1988); K. Miyamoto *et al.*, *Int. J. Cancer* **33**, 721 (1984); K. Okochi, H. Sato, Y. Hinuma, *Vox Sang.* **46**, 245 (1984).

19. We thank E. Chin, J. Q. Zhao, A. Diagne, S. Weitsman, and J. Breister for technical assistance; W. Aft and J. Stark for preparation of the manuscript; and J.-P. Allain for helpful comments on the manuscript. Supported in part by grants from the National Cancer Institute, the American Cancer Society, and the University of California–wide AIDS task force.

22 December 1988; accepted 27 February 1989

Scanning Tunneling Microscopy of Nucleic Acids

GIL LEE, PATRICIA G. ARSCOTT, VICTOR A. BLOOMFIELD, D. FENNELL EVANS

The scanning tunneling microscope (STM) has been used to measure properties of poly(rA)·poly(rU) and DNA, such as helical pitch, half-period oscillations that were interpreted as the alternation between the major and minor grooves, and interhelical spacing. Average pitches were measured by two-dimensional Fourier transforms and by topographic profiles along the fiber axes. Values were typically 7 percent less than standard dimensions of A-form RNA and B-form DNA fibers. This result is compatible with the mild dehydration that occurred under air-drying conditions. More extensive dehydration typically led to 19 percent shrinkage. Analysis of specific regions allowed local variations in helical pitch as small as 1 angstrom to be detected, thus demonstrating that the STM can visualize functionally significant modulations of nucleic acid structure.

THE STM HAS ENABLED REMARKable visualization of surface topography with a vertical resolution of 0.2 Å and horizontal resolution of 2 to 3 Å (*1*). The possibility of visualizing nucleic acids at this high resolution has major significance, since the binding of proteins and other aspects of gene regulation depend on structural variations at the level of 1 Å (*2*). Conventional electron microscopy allows the local structure of individual molecules to be discerned, unlike fiber diffraction or solution techniques that average over entire molecules and populations of molecules. The STM offers an additional advantage in that contrast is achieved by detection of sample height and work function variations, rather than by chemical treatments such as shadowing or staining. We report the use of the STM to measure the helical periodicities of air-dried double-stranded RNA and DNA molecules and in some cases to observe the alternation of major and minor grooves. Images of vacuum- and air-dried DNA were reported as early as 1984 by Binnig and Röhrer (*3*) and recently by Beebe *et al.* (*4*). However, these images were either obtained at low resolution or were so distorted that no reliable information could be obtained about helix dimensions. We show that nucleic acid dimensions and structural features can be quantitatively assessed and statistically analyzed by the STM, with small and reproducible corrections for hydration.

Calf thymus DNA (Sigma Chemical) and synthetic RNA, poly(rA)·poly(rU) (P-L Biochemicals, Milwaukee, Wisconsin) were purified and dissolved in a buffer of 1 m*M* sodium cacodylate, 10 m*M* NaCl, *p*H 7.4, at a concentration of about 7 μ*M* nucleotide phosphate. To promote lateral association by charge neutralization, the DNA was mixed for 2 hours with 200 μ*M* spermidine HCl or 100 μ*M* hexaamine cobalt (III); stable RNA fiber bundles were obtained without these trivalent cations. We found that bundles, rather than individual molecules, gave the most regular and reproducible images, perhaps because of mutual stabilization of neighboring molecules under dehydrating conditions. One-drop samples were deposited on freshly cleaved, highly oriented pyrolytic graphite (HOPG, Union Carbide grade ZYA), and were air-dried at room temperature.

A Nanoscope II (Digital Instruments, Inc., Santa Barbara, California) equipped with a 9-μm scan head made it possible to efficiently locate regions suitable for analysis but restricted the maximum magnification to areas 500 Å on a side (*5*). For most of the analysis, the digitized images were filtered to remove spike noise, narrow streaks, and the effects of sample tilt. Filtered and unfiltered images of poly(rA)·poly(rU) are shown in Fig. 1. Seven individual duplexes are readily discerned, and a repeat pattern is evident. A typical center-to-center distance between adjacent duplexes is 24.8 ± 0.8 Å (R-5 in Table 1), which is only slightly greater than the 21.3 Å diameter of RNA (*2*). The vertical profile of the cross section is consistent with the bundle being composed of a single layer of RNA helices (Fig. 1A).

The filtered vertical displacement profile (Fig. 1E) along a helical molecule oscillates uniformly with a period corresponding to the pitch of A-RNA. The unfiltered profile (Fig. 1F) shows the same pattern but also

G. Lee and D. F. Evans, Department of Chemical Engineering and Materials Science and Interfacial Sciences Center, University of Minnesota, 100 Union Street, S.E., Minneapolis, MN 55455.
P. G. Arscott and V. A. Bloomfield, Department of Biochemistry, University of Minnesota, 1479 Gortner Avenue, St. Paul, MN 55108.